Non-linear Optics III
(Phase-matching & frequency conversion)

P.E.G. Baird
MT 2011

Phase matching

In lecture 2, equation 22 gave an expression for the intensity of the second harmonic generated in a non-centrosymmetric crystal. The fundamental beam was taken as a plane wave travelling in the z-direction (*i.e.* $E_x = E_y = 0$).

$$I^{2\omega} = \frac{\omega^2(\chi^{SHG)})^2}{2n^{2\omega}(n^{\omega})^2c^3\varepsilon_0}(I^{\omega})^2 \left\{ \frac{\sin(\Delta kz/2)}{\Delta kz/2} \right\}^2 z^2 \tag{1}$$

where $I^{2\omega}$ has a phase determined by E^{ω}. When properly phase-matched $\Delta k = 0$ and $I^{2\omega}$ increases with z^2. The graph below shows the effect of phase-matching. With $\Delta k = 0$ the *sinc* function in curly brackets is equal to unity, and the second harmonic intensity increases with z^2; when not perfectly phase-matched the expression oscillates sinusoidally with a periodicity of $2\ell_c$ representing the fact that there is destructive interference between the second harmonic beam generated at different points in the crystal.

Index matching

We now need to understand how we achieve the phase-matching condition for a specific fundamental wavelength. For this we have to recall our picture of the index ellipsoid, and overlay the fundamental index variation with that of the second harmonic. The objective will be to see, if for example the fundamental wave propagates as the *ordinary* beam and the second harmonic as the *extraordinary* wave, there is a point at which $n_0^{\omega} = n_e^{2\omega}$. Thus we need both *birefringence* and *dispersion*. Analysis of the equations for the relevant ellipsoids reveals that the phase-matching angle is given by

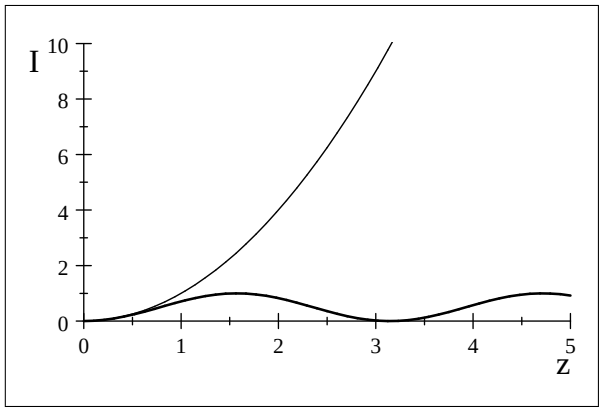

Figure 1: Variation of the intensity $I^{2\omega}$ with distance z

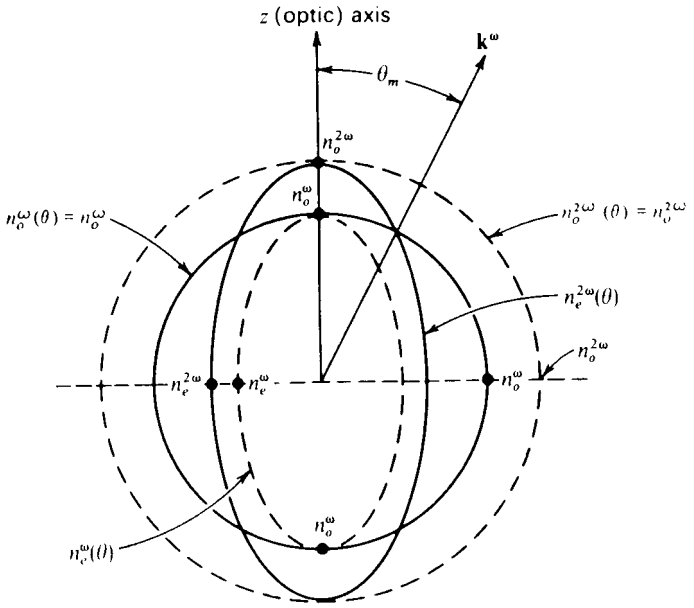

Figure 2: Refractive index variation for fundamental and second harmonic beams

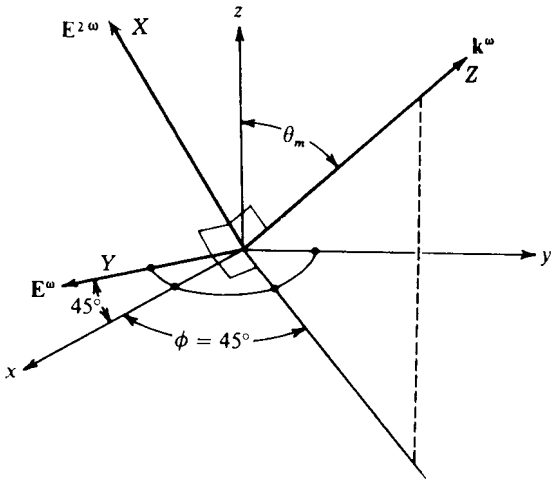

Figure 3: Directions of propagation for fundamental and SHG beams.

$$\theta_m = \cos^{-1}\left\{\frac{(n_0^{\omega})^{-2} - (n_e^{2\omega})^{-2}}{(n_0^{2\omega})^{-2} - (n_e^{2\omega})^{-2}}\right\}^{\frac{1}{2}} \tag{2}$$

As an example consider frequency doubling in ADP. The polarisation using equation 11 of lecture 1 is

$$P_i^{2\omega} = 2d_{ijk}E_j^{\omega}E_k^{\omega} \tag{3}$$

and given the symmetry of the crystal we have that

$$d_{14} = d_{25} \neq d_{36} \tag{4}$$

If Kleinman's conjecture [1] is invoked this reduces further since then

$$d_{14} = d_{36} \tag{5}$$

so that there is only one independent coefficient for SHG.

For the second harmonic to propagate as the extraordinary wave $P_x^{2\omega} = P_y^{2\omega} = 0$. Thus the relevant non-linear coefficient is

$$P_z^{2\omega} = 2d_{36}E_x^{\omega}E_y^{\omega} \tag{6}$$

The second harmonic intensity therefore maximises if :
(a) $\theta = \theta_m$;
(b) $\phi = 45^0$;
(c) the input beam is of low divergence and has a low bandwidth;
(d) the temperature is constant (since $n = f(T)$);
(e) the crystal is "short".

Walk-off

In the appendix of Lecture I we considered the propagation of light in a uniaxial crystal. We saw that, in general for the extraordinary ray, the direction of energy flow (Poynting's vector) and the wave-vector were not collinear; this leads the undesirable feature that the second harmonic beam (propagating as, say, the *extraordinary* beam) can *walk away* from the fundamental beam (propagating as the *ordinary* wave).

Straightforward geometry gives the walk-off angle for the negative uniaxial case, shown in the figure, as

$$\tan(\rho + \theta) = \left(\frac{n_o}{n_e}\right)^2 \tan\theta \tag{7}$$

Focussed Beams

The foregoing discussion has been restricted to the case of incident plane waves. While this makes the analysis relatively simple it does not in general describe the

[1] In most crystals there is no hysteresis in the dependence of P on E, i.e. P is single-valued. Furthermore there is no physical significance that can be attached to the exchange of labels of the two input fields so that $d_{i(jk)} = d_{i(kj)}$ and two subscripts suffice. However, there is a further "symmetry" consideration known as Kleinman's conjecture. For the case of a lossless medium only, the d coefficients which are related by a simple re-arrangement of the order of the subscripts are equal, *i.e.* $d_{yyx} = d_{yxy}$, thus, *e.g.*, $d_{12} = d_{26}$; $d_{36} = d_{14}$

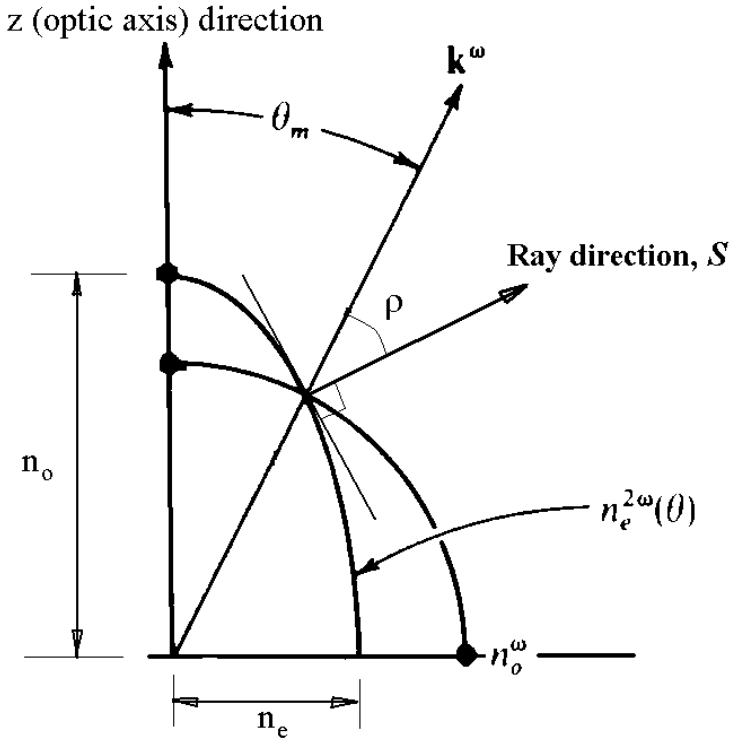

Figure 4: The wave-vector **k** and the direction of **S** are not collinear

situation encountered in practice where much greater conversion efficiency is achieved using focussed beams. Clearly this means that input arrives with a range of angles and with an intensity which varies along the propagation direction. Increasing the crystal length will then produce diminishing returns as the beam diverges either side of its focus. In practice this means matching the crystal length, L, to the confocal focus (Rayleigh length) of the beam $2z_0 = 2(\pi\omega_0^2 n/\lambda)$, *i.e.* to the distance over which the beam waist increases by a factor of $\sqrt{2}$. However, too tight a focus may lead to losses due to angular phase-mismatching. The 45^0, $z-$cut arrangement for the crystal gives the greatest angular tolerance for a given material, but of course this will only be useful if phase-matching can be achieved for the wavelength of interest by temperature tuning. Also for crystal cuts other than this, the issue of *walk off* has to be considered; the vectors S and k will no longer be collinear and the second harmonic beam will walk away from the fundamental beam producing it.

Depleted Input Beam

Once again the foregoing analysis has made one important assumption, namely that the fundamental beam is not significantly depleted in the doubling process. Thus, for high peak powers where high conversion efficiency can be achieved reduction in the fundamental intensity with distance through the crystal may become significant. In this case it may be shown for the perfectly phase-matched case ($\Delta k = 0$) that

$$\frac{I^{2\omega}}{I^{\omega}} = \tanh^2[\frac{\kappa L}{2}] \tag{8}$$

where κ is the single coupling parameter in the problem which is given by

$$\kappa^2 = 8d^2 \left(\frac{\mu_0}{\varepsilon_0}\right)^{3/2} \frac{\omega^2 I^{\omega}(0)}{n^{2\omega}(n^{\omega})^2} \tag{9}$$

[To do this you will need to solve the two coupled Helmholtz equations - see Lecture 2 and *Saleh & Teich*]

Note that when $\frac{\kappa L}{2} << 1$ so that $\tanh x \sim x$ we obtain

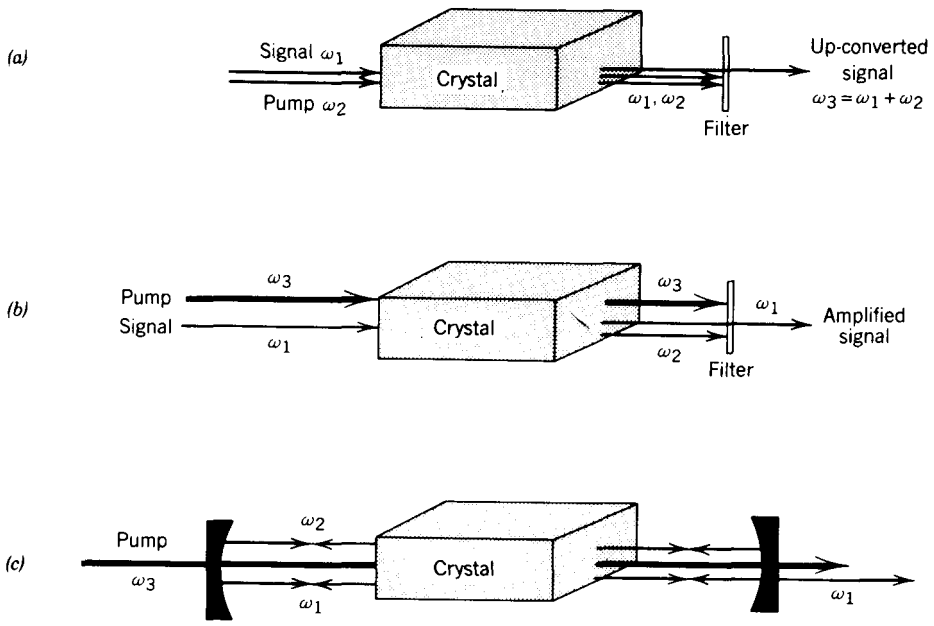

Figure 5: Examples of parametric processes

$$\frac{I^{2\omega}}{I^{\omega}} = 2d^2 \left(\frac{\mu_0}{\varepsilon_0}\right)^{3/2} \frac{\omega^2 I^{\omega}(0) L^2}{n^{2\omega}(n^{\omega})^2} \tag{10}$$

This is to be compared with equation (1) remembering $d \equiv \frac{1}{2}\varepsilon_0 \chi^{SHG}$ and $\Delta k = 0$.

Parametric processes

Let the time-varying optical field be described by,

$$E(t) = \mathrm{Re}\{E(\omega_1)\exp(-i\omega_1 t) + E(\omega_2)\exp(-i\omega_2 t)\} \tag{11}$$

The non-linear polarisation $P_{NL} = 2dE(t)^2$ now contains components at five frequencies: 0, $2\omega_1$, $2\omega_2$, $\omega_+ = \omega_1 + \omega_2$, $\omega_- = \omega_1 - \omega_2$ with amplitudes

$$\begin{aligned}
P_{NL}(0) &= d\,[|E(\omega_1)|^2 + |E(\omega_2)|^2] && (12)\\
P_{NL}(2\omega_1) &= d\,E(\omega_1)E(\omega_1) && (13)\\
P_{NL}(2\omega_2) &= d\,E(\omega_2)E(\omega_2) && (14)\\
P_{NL}(\omega_+) &= 2d\,E(\omega_1)E(\omega_2) && (15)\\
P_{NL}(\omega_-) &= 2d\,E(\omega_1)E^*(\omega_2) && (16)
\end{aligned}$$

Thus if waves 1 and 2 are plane waves then $E(\omega_1) = A_1 \exp(i\mathbf{k}_1.\mathbf{r})$ and $E(\omega_2) = A_2 \exp(i\mathbf{k}_2.\mathbf{r})$ and equation 15 gives $P_{NL}(\omega_+) = 2d\ A_1 A_2 \exp(i\mathbf{k}_3.\mathbf{r})$ where $\omega_1 + \omega_2 = \omega_3$

and $\mathbf{k}_1 + \mathbf{k}_2 = \mathbf{k}_3$

Equivalently we may say *energy* conservation requires $\omega_1 + \omega_2 = \omega_3$ (in the cases of SHG and up-conversion); $\omega_1 = \omega_3 - \omega_2$ (in the case of down-conversion), while *momentum* conservation requires the vector equation $\mathbf{k}_1 + \mathbf{k}_2 = \mathbf{k}_3$ to be satisfied.

Single Photon Sources

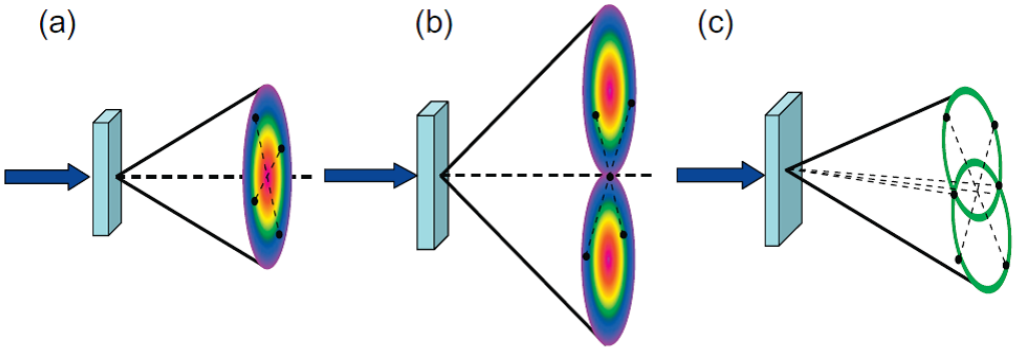

Figure 6: Parametric-down conversion schemes (a) Type-I; (b) Type-II and (c) correlated pairs at certain positions leading to polarisation-entangled states (See reference [1])

We make here a connection between parametric down-conversion and single-photon states. Single photons are in many ways ideal carriers for quantum information due to their negligible interaction with the environment. Some proposed architectures for large quantum networks rely on "stationary" atoms or ions as information processing nodes and single photons to transmit information in optical fibres along large distances. In spontaneous down-conversion, photon pairs can be created; the nonlinear interaction of a pump laser photon with the crystal occasionally splits one high-frequency photon into two lower-frequency ones - the signal and the idler photons. The process is said to be degenerate if $\omega_i = \omega_s = \omega_p/2$ and non-degenerate otherwise.In general the two photons generated travel in different directions but under certain condition they may exit collinearly, in the same direction as the pump. The down-conversion process is called type-I if the signal and idler have identical polarisations; with type-II phase-matching the size and idler are orthogonally polarised.

Worked Example

The two-photon transition (1s-2s) in atomic hydrogen requires radiation at 243nm. We consider here the possibility of generating this radiation by frequency *summing* in a crystal of KDP using 351nm radiation from an argon ion laser and tunable radiation at 789nm from an oxazine dye laser [2,3]. First the crystal. KDP is somewhat harder than ADP and good quality crystals can easily be grown and the faces polished to a very high optical quality. Both ADP and KDP are negative uniaxial crystals of the tetragonal $\bar{4}2$m class. The piezoelectric tensor is thus of the form

$$\begin{pmatrix} P_x \\ P_y \\ P_z \end{pmatrix} = \begin{pmatrix} \cdot & \cdot & \cdot & \bullet & \cdot & \cdot \\ \cdot & \cdot & \cdot & \cdot & \bullet & \cdot \\ \cdot & \cdot & \cdot & \cdot & \cdot & \bullet \end{pmatrix} \begin{pmatrix} E_x^2 \\ E_y^2 \\ E_z^2 \\ 2E_yE_z \\ 2E_xE_z \\ 2E_xE_y \end{pmatrix} \tag{17}$$

For type I phase-matching the fundamental beam propagates as the ordinary wave (see above). The generated UV is therefore produced by (see figure 5),

$$P_z^{'} = P_z \sin\theta = 2\varepsilon_0 d_{36} E_0^2 \sin\theta(\cos\phi \times \sin\phi) \tag{18}$$

$$= \varepsilon_0 d_{36} E_0^2 \sin\theta \sin 2\phi \tag{19}$$

This clearly maximizes at $\phi = 45^0$ At $\theta = 90^0$ and $\phi = 45^0$ the effective non-linear coefficient is $d_{eff} = d_{36}$ $(= 0.47 \times 10^{-12}\text{mV}^{-1})$. For this arrangement there is no walk off and the angular tolerance is highest.

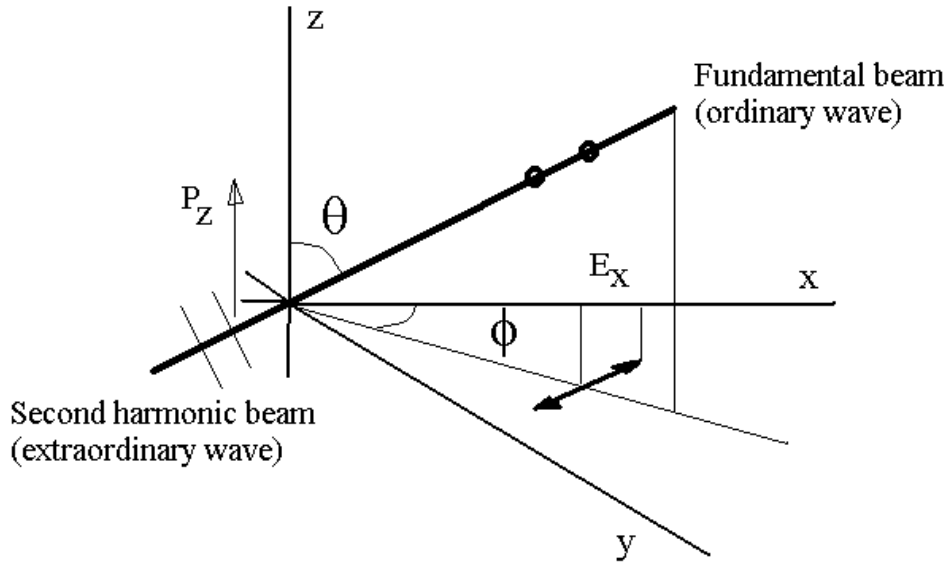

Figure 7: Direction of fundamental beam with polarisation projected in xy-plane

Phase-matching.

Conservation of energy requires.

$$\frac{1}{243} - \frac{1}{351} = \frac{1}{\lambda_2} \tag{20}$$

hence $\lambda_2 = 789$nm. The refractive indices must now satisfy the equation,

$$\frac{n_0}{351} + \frac{n_0'}{789} = \frac{n_e}{243} \tag{21}$$

Refractive index data for both KDP and ADP are given by Zernike in *J.Opt.Soc.Am.* 54, 1215, 1964. For room temperature, we find $n_0(351) = 1.53236$; $n_0'(790) = 1.50226$; $n_e(243) = 1.522638$. Phase-matching at room temperature, therefore, gives

$$\frac{n_0}{351} + \frac{n_0'}{789} = \frac{1}{159.558} \qquad \left(cf. \frac{1.522638}{243} = \frac{1}{159.5914} \right) \tag{22}$$

i.e. very close ! Exact phase-matching at room temperature can be obtained by angle-tuning to bring the extraordinary refractive index necessary to produce the exact k_3 wave vector. Thus,

$$\theta = \sin^{-1} \left\{ \frac{n_e(\lambda_3)}{n_e^\theta(\lambda_3)} \sqrt{\frac{n_0^2(\lambda_3) - n_e^\theta(\lambda_3)^2}{n_0^2(\lambda_3) - n_e^2(\lambda_3)}} \right\} \tag{23}$$

since,

$$\frac{1}{n_e^2(\theta)} = \frac{\cos^2\theta}{n_o^2} + \frac{\sin^2\theta}{n_e^2} \tag{24}$$

This gives $\theta = 85.5^0$, *i.e.* very close to 90^0. Alternatively phase-matching at $\theta = 90^0$ can be achieved by temperature tuning. Data for the refractive index variation with temperature are given by Vishnevskii & Stefanski (Opt. & Spec. 20, 195, 1966). and by Phillips (Opt. Soc. Am. 56, 629, 1966).

For temperature phase-matching

$$\left(\frac{n_0}{351} + \frac{n_0'}{789} - \frac{n_e}{243} = \Delta T \times \left\{ \left(\frac{dn_0/dT}{351} \right)_{351} + \left(\frac{dn_0/dT}{790} \right)_{790} - \left(\frac{dn_e/dT}{243} \right)_{243} \right\} \right) \tag{25}$$

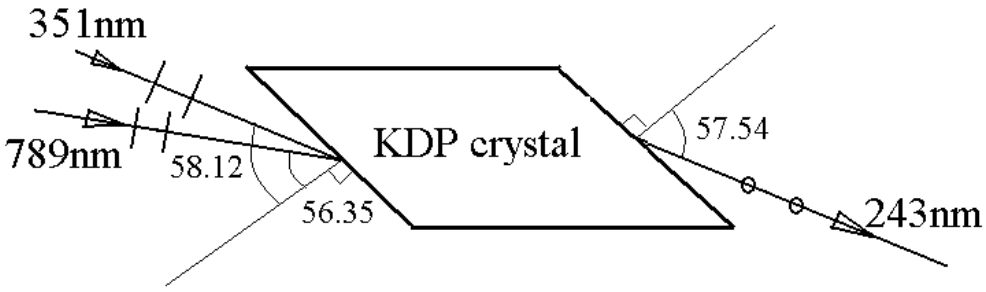

Figure 8: A Brewster-cut crystal minimises reflection for the input laser beams.

Hence ΔT. For intra-cavity mixing or in general for low loss the crystals can be cut so as to have near Brewster faces for the fundamental beams. For KDP we find Brewter's angle ($\tan^{-1} n$) for 789nm to be 56.35^0; for 351nm 58.12^0.The UV radiation at 243nm will emerge at 57.54^0 but in this case the polarisation is orthogonal (it propagates as the extraordinary beam) so there will be a single-pass Fresnel loss.

References

[1] *Single-Photon Sources,* B. Lounis and M. Orrit, **Reports in the Progress of Physics 68**, 1129-1179, 2005

[2] *Generation of continuous-wave radiation near 243 nm by sum-frequency mixing in an external ring cavity,*B. Couillaud,* L. A. Bloomfield, and T. W. Hansch **Optics Letters 8,** 259-261, 1983

[3] *High Power sum-frequency generation near 243nm using two insecting enhancement cavities* B. Couillaud, T.W. Hansch, and S.G. MacLean, **Optics Communications 50**, 127, 1984